J. Comp. Path. 2010, Vol. 142, 157–169

ELSEVIER
www.elsevier.com/locate/jcpa

Characterization and Time Course of Pulmonary Lesions in Calves after Intratracheal Infection with *Pasteurella multocida* A:3

M. P. Dagleish*, J. Finlayson*, C. Bayne*, S. MacDonald*, J. Sales† and J. C. Hodgson*

** Moredun Research Institute, Pentlands Science Park, Bush Loan, Penicuik, Near Edinburgh and † Biomathematics & Statistics Scotland, James Clerk Maxwell Building, The King's Buildings, University of Edinburgh, Edinburgh, UK*

Summary

Pasteurella multocida A:3 is a common cause of suppurative bronchopneumonia in calves and results in significant production losses and mortality. Here we describe the lesions in three calves at each of four time points (1 day and 4, 7 and 10 days) after experimental intratracheal infection with approximately 1×10^9 colony-forming units of *P. multocida* A:3 Moredun Research Institute (MRI isolate 671/90). Equivalent age- and time-matched sham-dosed negative control animals were also studied. Infected calves developed significantly elevated mean rectal temperatures ($P < 0.001$) and respiratory rates ($P < 0.001$) compared with negative control animals. Extensive consolidation of multiple lung lobes was present on each of the day/s post-infection (dpi). Histologically, large numbers of alveoli contained either or both polymorphonuclear neutrophils (PMNs) and oedema fluid (1 dpi). At 4 dpi a severe fibrinosuppurative bronchopneumonia had developed. At this time, PMNs and macrophages formed focal lesions containing central necrotic and mineralized debris, while the interlobular septa were severely distended by oedema. Early abscess formation was present in the lung parenchyma at 7 dpi and many of the interlobular septa were thrombosed. At 10 dpi abscesses within the lung parenchyma were mature and comprised of central necrosis with surrounding layers of PMN, macrophages and fibrous tissue. This study describes, for the first time, the commencement, nature and progression of lesions in bovine pneumonic pasteurellosis caused by *P. multocida* A:3 and provides the foundations for further investigation of the pathogenesis of this disease in cattle.

Keywords: cattle; *Pasteurella multocida*; pathology; pneumonia

Introduction

Pasteurella multocida is a gram-negative bacterium found on the epithelium of the upper respiratory tracts in apparently healthy animals of several different species (Biberstein, 1990). Isolates are categorized into five serogroups (A, B, D, E and F) based on capsular antigens and by somatic antigens into 16 serotypes (Rimler and Rhoades, 1989). Serotype A:3 is associated with severe suppurative bronchopneumonia in calves (Confer *et al.*, 1996) resulting in significant production losses and mortality (Dalgleish, 1989; Weekley *et al.*, 1998). In the UK, bovine pneumonic pasteurellosis due to infection with *P. multocida* has increased in prevalence in cattle such that from 2001 to 2005 it was the most frequently diagnosed cause of bovine bacterial pneumonia and exceeded the number of outbreaks caused by *Mannheimia haemolytica* (Veterinary Laboratories Agency, 2007). The pathology of pneumonic pasteurellosis caused by *M. haemolytica* has been well described in both naturally acquired (Caswell and Williams, 2007) and experimental (Jericho, 1989) infections, including the lesions at multiple time points (Allan *et al.*, 1985). However, reports of the pathology of both natural and experimental infections in calves with *P. multocida* A:3 (Gourlay *et al.*, 1989; Dowling *et al.*, 2002, 2004; Mathy *et al.*, 2002; Ishiguro *et al.*, 2005; Caswell and Williams, 2007) have described only the lesions at a single time point after their initiation, and this lack of a detailed description of the commencement,

Correspondence to: M. P. Dagleish (e-mail: mark.dagleish@moredun.ac.uk).

0021-9975/$ - see front matter
doi:10.1016/j.jcpa.2009.10.015

nature and progression of lesions in bovine pneumonic pasteurellosis caused by *P. multocida* has been highlighted (Caswell and Williams, 2007).

The aim of the present study was to describe the clinical responses and gross and microscopical lesions that develop during the course of experimental pneumonic pasteurellosis in calves over a 10-day period after intratracheal infection with *P. multocida* A:3. Additionally, the distribution of *P. multocida* bacteria within the lesions, as determined by specific immunohistochemical labelling of lung tissue and selected pulmonary lymph nodes, is described.

Materials and Methods

Animal Procedures

Twenty-four male Holstein-Friesian calves free of *P. multocida* were used in the study. At the farm of origin nasal swabs were taken from calves within 3 days of birth. These were streaked over agar plates containing 5% sheep blood and vancomycin (final concentration 10 μg/ml to prevent growth of gram-positive bacteria) in agar base No. 2 (Oxoid, Basingstoke, UK) and cultures were examined for the presence of *P. multocida* by colony morphology and polymerase chain reaction (PCR; Townsend *et al.*, 1998). Calves that tested negative for the presence of *P. multocida* were transferred to the Moredun Research Institute and held in open pens for the duration of the experiment. At approximately 7 weeks of age calves were weaned from a liquid milk diet on to hay and mixed pellets. They were allocated randomly to two groups each of 12 animals and allowed to acclimatize to their surroundings and each other. Access to veterinary care was available at all times and calf health and well-being was assessed regularly each day so that any necessary treatment might be given with minimal delay.

Each group of calves was housed in a separate airspace. Calves in group 1 (G1) were each infected with approximately 10^9 colony-forming units (cfu) of *P. multocida* A:3 Moredun Research Institute (MRI isolate 671/90) diluted in 300 ml of pre-warmed sterile phosphate buffered saline (PBS, pH 7.4, 0.33 M) given intratracheally via a fibreoptic endoscope at 8 weeks of age (day 0) as described previously (Dowling *et al.*, 2002). Calves in group 2 (G2) were each sham-infected with 300 ml of pre-warmed sterile PBS given in the same way as above to provide age and time-matched negative control data. Calf rectal temperatures, respiratory rates and general demeanour (normal, dull or depressed as a score of 0, 1 or 2, respectively) were recorded daily prior to infection, immediately before and every 4 h after infection on day 0 and twice daily thereafter. Scheduled post-mortem (PM) examinations were performed on three calves from each of G1 and G2 at 1, 4, 7 and 10 day/s post-infection (dpi). All experimental protocols involving animals were approved by the Moredun Research Institute Animal Experiments and Ethical Review Committee and were authorized under the UK Animals (Scientific Procedures) Act 1986.

Preparation of Infection and Sham Doses

To ensure uniformity of infection to calves in G1, all doses were prepared using glycerol stocks from a single culture broth of *P. multocida* serotype A:3 (MRI isolate 671/90) inoculated into 10 ml Oxoid nutrient broth (NB) for 16 h static incubation at 37°C followed by subculture of 0.5 ml aliquots inoculated into fresh 10 ml aliquots of NB, incubated for 3.5 h at 37°C with shaking (140 rpm). Aliquots of culture (approx. 1 ml) were added to 300 ml of pre-warmed sterile PBS as previously described (Dowling *et al.*, 2002) to provide an estimated infection dose of 10^9 cfu of *P. multocida*. The actual mean dose was 1.37×10^9 cfu, determined retrospectively from viable counts after spotting metered amounts onto sheep blood agar (SBA; blood agar base [Oxoid] containing 5% [v/v] sheep blood).

Necropsy Examination

Calves for necropsy examination were killed by intravenous injection of pentobarbitone sodium B.P. (approx. 200 mg/kg; Rhone Merieux, UK) followed immediately by exposure and clamping, with artery forceps, of the cervical trachea prior to severing the blood vessels of the neck. The thoracic cavity was opened by removal of the sternum and adjoining distal ribs to allow assessment of the presence of pleurisy (scored between 0 and 3; 0 = no pleurisy and 3 being the most severe). Subsequently, the trachea, heart and lungs were removed together to allow assessment of gross lesions by visual examination and by palpation and calculation of the percentage of affected whole lung surface area as described previously (Gilmour *et al.*, 1983; Dowling *et al.*, 2002). Representative samples of tissue from the right and left cranial, right middle, right and left caudal and accessory lung lobes were placed into 10% neutral buffered formalin. Selected lymph nodes (left and cranial bronchial and mid and caudal mediastinal), which could be recognized consistently in all calves, were removed whole and dissected free from all adjacent material prior to being weighed and then fixed as above.

Bacteriological Examination

Small samples (approximately 1 cm cubes) of lung parenchyma were taken from four pre-selected sites (cranial, right middle, accessory and caudal lobe) and each was homogenized in 9 ml peptone water and diluted in 10-fold steps to 10^{-6}. Aliquots (10 µl) of each dilution from 10^{-6} to 10^{-2} were applied to SBA plates and incubated at 37°C for 16–20 h. Viable counts were determined and expressed as cfu/g of tissue.

Histopathology

All formalin-fixed tissue samples were prepared for microscopical examination by standard techniques (dehydrated through graded alcohols, embedded in paraffin wax, sectioned [5 µm], mounted on glass microscope slides and stained with haematoxylin and eosin [HE]). Duplicate sections from the lung samples were also stained with elastic van Gieson to aid differentiation of pulmonary from bronchial arteries. The pathological morphology of any histological lesions was recorded and an overall grading for severity was assigned to each sample (0, no significant lesions; 1, perceptible; 2, mild; 3, moderate; 4, severe; and 5, very severe).

Immunohistochemistry (IHC) for P. multocida *A:3*

A further tissue section from all samples was mounted on Superfrost™ slides (Menzel-Gläser, Braunschweig, Germany) and subjected to IHC with polyclonal rabbit antiserum raised against formalin-killed, whole cell preparations of the infection strain of *P. multocida* A:3. Briefly, 0.5 ml of a static 16 h culture of *P. multocida* A:3 (MRI isolate 671/90) in NB at 37°C was subcultured into 50 ml NB and placed on a rotary shaker for 4 h at 37°C. A total of approximately 10^9 cfu cells was then centrifuged at 2,000 g for 30 min at 20°C and killed by resuspending in 0.3% (v/v) formalin overnight at 4°C. Dead bacteria were washed in sterile PBS to remove the formalin, centrifuged at 2,000 g for 20 min at 20°C and resuspended in 50 ml PBS at 1×10^6 cfu/ml prior to storage at 4°C. A sample of the formalin-killed *P. multocida* A:3 suspension was streaked onto SBA at weekly intervals throughout the inoculation procedure to check for bacterial contaminants. A 6-month-old rabbit was given 0.5 ml of the killed bacterial suspension subcutaneously and then 1.0 ml and 2.0 ml by the same route 2 and 5 days later, respectively. Subsequent to this the rabbit was given 2.0 ml of the killed bacterial suspension via the intravenous route every 3 days on six occasions. The rabbit was killed 10 days after the last inoculation and exsanguinated. Serum was stored in aliquots at −20°C until required.

Microscopical sections for IHC were dewaxed in xylene and rehydrated through graded alcohols to 95% alcohol prior to quenching endogenous tissue peroxidase activity with H_2O_2 3% in methanol (v/v) for 20 min. Subsequent to this, slides were washed in water for 5 min and then transferred to PBS containing 0.05% v/v Tween 20 (PBS-T). Non-specific antigen binding was blocked by incubation with 25% normal goat serum (Vector Laboratories, Peterborough, UK) diluted in PBS-T for 30 min at room temperature. Rabbit anti-*P. multocida* A:3 antiserum diluted 1 in 2,000 in PBS-T was applied; the slides were incubated overnight at 4°C then washed in PBS-T (3 × 5 min). Anti-rabbit IgG conjugate (EnVision™ System-HRP; code K4011; Dako UK Ltd, Ely, UK) was added for 30 min at room temperature, slides were washed in PBS-T (3 × 5 min) and incubated for 8 min with 3,3′-diaminobenzidine (DAB) chromagen (EnVision™ System-HRP) prior to being washed in water and counterstained with haematoxylin. Negative control slides were prepared using non-immunized rabbit serum. Slides were examined in blinded fashion for the presence and distribution of immunolabelling relative to histological lesions and a combined overall grading (0–5) for intensity and extent of labelling was assigned to each sample (0 = no significant immunolabelling, 5 = most severe).

Statistical Analyses

For the clinical responses (rectal temperature and respiration rate) a repeated measures model was fitted to the data with the lack of independence between successive measurements from the same animal modelled using a power model. Group (infected [G1] or control [G2]), day post-infection and group × day interaction were included in the model as categorical fixed effects. For the PM data (lung scores, lymph node scores, lymph node weights on a log scale and calf weights), linear mixed models were fitted to the data with group, day killed and the group × day interaction included as categorical fixed effects and calf as a random effect. Parameters in all of these models were estimated using the REML directive in GenStat 10th Edition. The differences in the proportions of animals in each group that had a maximum demeanour score of 0, 1 and 2, respectively, on the day of infection were assessed using a Fisher's exact test. Six immunohistochemical sections of the lung (one for each lung lobe) were scored for each animal and the mean score over these six areas was calculated for each animal and used in the subsequent analysis.

All of the control animals had zero scores in all areas. A one-way analysis of variance (ANOVA) was carried out for animals in the infected group using the day killed as a factor. IHC scores were recorded for four lymph nodes. The scores for the infected group (G1) were mainly zero and for G2 all zero, so the data were too sparse to satisfactorily carry out a one-way ANOVA. A two-way table was created which gave the number of animals on each day that had a mean score of either zero or greater than zero and a Fisher's exact test was carried out to determine whether the proportion of animals with a mean score of zero changed over time. As there was no evidence of systematic changes between the days of sampling in the percentage of consolidation present in the lungs, a Mann–Whitney test was used to investigate differences in the median percentages between the two groups. All analyses were carried out using GenStat 10th Edition apart from the Fisher's exact tests, which were carried out using the R computing environment.

Results

Clinical Responses of Calves to Infection

Calves in G1 and G2 differed significantly ($P < 0.001$) in their pattern of change of mean rectal temperature post-infection. Prior to infection the mean rectal temperatures standard deviation (±SD) for groups G1 and G2 were 38.6 ± 0.44 and 38.4 ± 0.34°C, respectively. The mean rectal temperature in G1 calves at 1 dpi increased and reached a peak of 40.2 ± 0.66°C by 12 h post-infection, and remained elevated for the duration of the experiment. The mean rectal temperature of G2 calves remained fairly constant throughout at 38.7 ± 0.32°C. Similarly, the pattern of mean respiratory rate of calves in G1 was significantly different ($P < 0.001$) from that of G2 in that it increased from 32 breaths per minute (bpm) prior to infection to a peak value of 87 bpm at 12 h post-infection compared with animals in G2 (31.5 bpm and 27.5 bpm at pre-infection and 12 h post-infection, respectively). Although the mean respiratory rate did decrease, somewhat variably, for G1 over the duration of the experiment, it remained consistently greater than that of G2. On the day of infection, in G1 a demeanour score of 2 was recorded for two animals and a score of 1 for another nine, whereas in G2 all of the calves had a demeanour score of zero ($P < 0.001$; Fisher's exact test). Subsequent to this, scores of either 1 or zero only were recorded in G1 and, in general, the proportion of calves in this group with zero scores increased after the day of infection; however, there were insufficient data to draw any firm conclusions about changes in demeanour over time. All calves in G2 had a demeanour score of zero at all times throughout the experiment.

Bacteriology of Lung Tissue

P. multocida A:3 was cultured from all four samples of lung tissue taken from all G1 calves except one, examined at 10 dpi, in which only the right middle lung lobe sample yielded growth (Table 1). In some calves there was considerable variability in cfu/g between individual lung samples (Table 1). No bacterial growth was present in any of the lung samples from calves in G2.

Gross Pathology

Lesions, when present, were confined to the thoracic cavity and, irrespective of day of examination, variable amounts of consolidation of the lung parenchyma were present in all G1 calves, but no significant consolidation was present in any G2 calf (Table 2). The consolidated areas were deep red, firm when palpated and well-demarcated, even at 1 dpi, and contained interlobular septa that were oedematous (Fig. 1a). At 7 dpi nodules of pus were visible within the parenchyma (Fig. 1b) and at 10 dpi similar subpleural lesions, which were more clearly demarcated, deformed the surface of the lung. In affected animals pleurisy was present from 4 dpi onwards as fibrin deposits on the visceral and parietal pleura, which, with time, increased in area affected and changed in morphology from gelatinous to fibrinous then fibrous adhesions between lung tissue and the thoracic wall (Table 2). At 10 dpi several of the

Table 1
Bacterial count of *P. multocida* A:3 from the lungs of infected calves

Calf ID (dpi)	*Lung pool (cfu/g)*			
	Right cranial	*Right middle*	*Accessory*	*Caudal*
1 (1)	1.46×10^3	7.57×10^5	3.70×10^3	1.12×10^7
2 (1)	5.14×10^5	1.23×10^7	2.11×10^6	7.51×10^5
3 (1)	4.94×10^3	2.29×10^5	3.95×10^2	4.76×10^3
4 (4)	4.17×10^3	8.72×10^2	6.07×10^4	8.92×10^6
5 (4)	6.90×10^3	5.54×10^3	6.76×10^3	9.54×10^5
6 (4)	6.52×10^3	4.31×10^3	4.04×10^2	4.46×10^6
7 (7)	3.01×10^2	9.46×10^2	5.49×10^2	5.00×10^2
8 (7)	4.18×10^4	1.52×10^6	2.76×10^5	3.46×10^4
9 (7)	6.93×10^2	6.38×10^2	8.10×10^2	6.74×10^2
10 (10)	0	4.74×10^6	0	0
11 (10)	5.55×10^6	2.55×10^6	3.25×10^3	4.74×10^5
12 (10)	6.12×10^4	1.57×10^6	1.13×10^7	3.86×10^4

dpi, day/s post-infection; cfu/g, colony-forming units per gram.
Data are from four lung lobes from calves in G1; no organisms were recovered from calves in G2.

Table 2
Gross lung pathology

Calf ID	*Group*	*dpi*	*Consolidation (%)*			*Pleurisy score*	*Notes*
			Dorsal	*Ventral*	*Mean*		
1	G1	1	20.3	24.1	22.0	0	–
2	G1	1	6.0	12.0	9.0	0	–
3	G1	1	9.0	12.0	10.5	0	–
4	G1	4	34.4	46.6	40.5	1	Surface fibrin present
5	G1	4	24.5	38.8	31.4	2	Ventral gelatinous adhesions
6	G1	4	28.0	27.0	27.5	1	Surface fibrin present
7	G1	7	29.1	29.3	29.2	2	Ventral gelatinous adhesions
8	G1	7	28.0	35.5	31.7	3	Ventral fibrinous adhesions
9	G1	7	8.0	8.0	8.0	0	–
10	G1	10	13.7	18.8	16.2	0	–
11	G1	10	21.0	31.0	26.0	3	Mature fibrous adhesions
12	G1	10	37.0	30.0	33.5	3	Mature fibrous adhesions
13	G2	1	0.8	1.5	1.1	0	–
14	G2	1	1.0	0	0.5	0	–
15	G2	1	0	0	0	0	–
16	G2	4	0	0	0	0	–
17	G2	4	0	0	0	0	–
18	G2	4	0	0	0	0	Slight haemorrhage
19	G2	7	0	0	0	0	–
20	G2	7	0	0	0	0	–
21	G2	7	0.5	0	0.25	0	–
22	G2	10	1.0	0	0.5	0	–
23	G2	10	1.0	1.0	1.0	0	Mature abscess and adhesions
24	G2	10	0	0	0	0	–

G1, group 1; G2, group 2; dpi, day/s post-infection.
Amount of consolidation present in the lungs from each calf is represented as a percentage of ventral and dorsal surfaces affected. Presence and severity of pleurisy (scored between 0 and 3, where 0 is no pleurisy and 3 is most severe).

adhesions present were of a mature fibrous nature, firm and difficult to break down. Mean pulmonary lymph node weights from G1 calves were significantly greater ($P \leq 0.001$) than those from G2 calves (Table 3), with mean weights of each lymph node being approximately 2.5 times heavier in G1 compared with G2.

Histopathology

The three G1 calves subjected to necropsy examination at 1 dpi had microscopical lesions of severe suppurative bronchopneumonia in the right and left cranial, right middle and accessory lung lobes and, in a single calf, the right caudal lung lobe (Table 4). Lesions, which were similar in all lung lobes, were comprised of a severe and widespread infiltration of polymorphonuclear neutrophils (PMNs) into the alveolar and bronchiolar airspaces, often filling them completely, and extensive yet scattered areas of alveolar oedema that frequently filled the alveoli. Alveolar infiltration with PMNs and alveolar oedema occurred as a patchwork of either one or the other change in the affected lung parenchyma, but sometimes as mixtures of the two processes (Fig. 2a). The alveolar septa in affected areas of lung frequently appeared congested and sometimes oedematous. At 1 dpi, scattered amongst the PMNs in the alveoli, there were a number of mononuclear inflammatory cells. These had large basophilic nuclei that were open and pale and surrounded by variable amounts of pleomorphic cytoplasm typical of macrophages. A similar cellular infiltration of the alveoli and bronchioles was present in the region of some small bronchi. However, only small numbers of PMNs were present in large bronchi, usually in aggregates in the lumen adjacent to the respiratory epithelium. Haemorrhages were scattered throughout affected alveoli. The deep lymphatic vessels adjacent to pulmonary arterioles were frequently distended. Bronchial-associated lymphoid tissue (BALT) appeared well developed, although some of these structures appeared mildly depleted. PMNs infiltrated the interlobular septa, especially adjacent to the interlobular lymphatics, which were dilated, sometimes severely so (Fig. 2b). In some of the latter there was a fine lacework of fibrin. Mononuclear inflammatory cells, indistinguishable from those in the bronchioles and

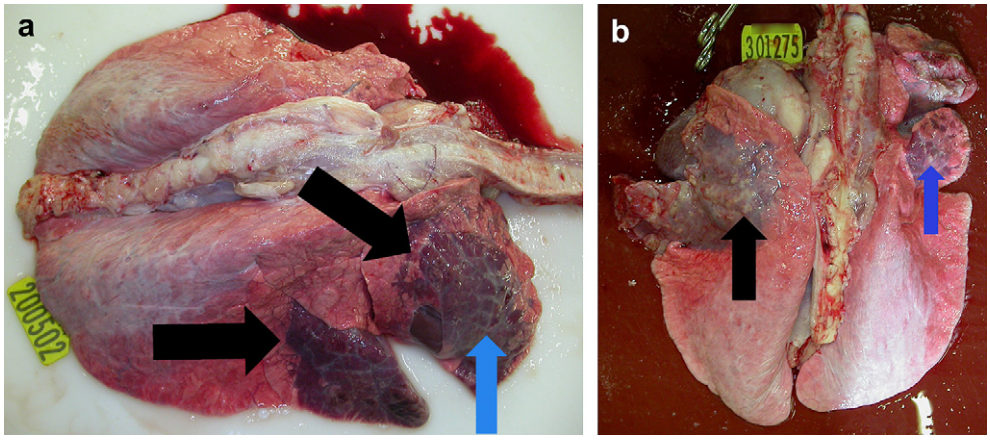

Fig. 1. (a) Dorsal surface of lungs at 1 dpi with *P. multocida* A:3 pneumonia. Clearly demarcated areas of deep red consolidation are present (black arrows) in the right cranial and middle lung lobes in this animal and many of the interlobular septa in the affected areas are oedematous (blue arrow). (b) Dorsal surface of lungs at 7 dpi with *P. multocida* A:3 pneumonia. Multiple coalescing areas of pus are present in the subpleura in the affected consolidated left anterior lung lobe (black arrow) and to a lesser extent in the right anterior lung lobe also (blue arrow).

alveoli, were present within the aggregations of PMNs infiltrating the interlobular septa and, in greater numbers, deep within the interstitial tissue of the interlobular septa away from the lymphatics. Mild lesions only were present in the right and left caudal lung lobes examined, with the exception of a single right caudal lung lobe (Table 4).

Table 3
Weights of four consistently recognizable pulmonary lymph nodes and calf weight at time of necropsy examination

Calf ID (group)	*dpi*	*Left bronchial (g)*	*Cranial bronchial (g)*	*Mid-mediastinal (g)*	*Caudal mediastinal (g)*	*Calf weight (kg)*
1 (G1)	1	8.2	3.0	3.6	8.5	N/A
2 (G1)	1	3.2	1.7	3.1	12.2*	62.0
3 (G1)	1	2.0	0.7	1.6	6.4	68.8
4 (G1)	4	17.6	2.9	5.8	22.1	94.6
5 (G1)	4	5.5	1.9	5.7	13.6	85.6
6 (G1)	4	5.9	1.2	4.0	19.6	81.0
7 (G1)	7	14.4*	5.3*	3.3*	19.4	97.2
8 (G1)	7	15.7*	7.1	4.9*	16.0	80.0
9 (G1)	7	6.9	1.6	3.9	6.2	77.0
10 (G1)	10	8.2*	3.8*	3.6*	10.8*	86.6
11 (G1)	10	5.8	3.9	3.3*	13.5	94.6
12 (G1)	10	9.4*	0.9	5.6*	6.8*	79.4
13 (G2)	1	2.9	0.8	1.6	5.0	N/A
14 (G2)	1	2.0	1.2	1.5	5.3	N/A
15 (G2)	1	2.5	1.0	0.7	6.5	N/A
16 (G2)	4	7.6	0.5	1.8	8.3	96.8
17 (G2)	4	3.5	1.3	1.5	5.0	95.4
18 (G2)	4	1.6	0.6	1.2	3.8	67.1
19 (G2)	7	2.4	0.4	0.9	3.9	95.6
20 (G2)	7	2.3	0.8	1.3	3.8	87.4
21 (G2)	7	3.0	0.4	0.9	4.0	83.4
22 (G2)	10	3.9	0.9	1.7	8.0	107.6
23 (G2)	10	4.1	1.3	2.0	5.9	94.4
24 (G2)	10	4.0	1.6	1.0	5.1	90.4

G1, group 1; G2, group 2; dpi, day/s post-infection; N/A, not available.
*Perceptible positive immunolabelling for *P. multocida* A:3.

In all three G1 calves examined at 4 dpi there were histological lesions of severe fibrinosuppurative bronchopneumonia in one or more lung lobes. The lung lobes affected most consistently were the right middle and accessory lobes, followed by the right and left cranial lobes. The effect on the caudal lobes was less severe, although more than that observed in G1 calves examined at 1 dpi (Table 4). All of the microscopical lesions described at 1 dpi were present; additionally, there was fibrin present within the alveoli and fewer cells in the airspaces in the centres of the lesions. Delineation of lesions was more obvious due to a layer of intense cellularity comprised of both PMNs and mononuclear inflammatory cells (Fig. 3). The alveolar septa in the centres of the lesions were swollen, congested and often haemorrhagic and many of the inflammatory cells were mononuclear with large nuclei and abundant foamy cytoplasm characteristic of activated macrophages. In the centres of some of the lesions there were numerous PMNs and macrophages, and alveolar septa were necrotic and mineralized in some instances. Peripheral to the layer of intense cellularity, many of the alveoli contained large amounts of fibrin, scattered inflammatory cells and multinucleate giant cells. The lymphatics adjacent to pulmonary arterioles were distended and contained large amounts of fibrin. A consistent finding was massive oedema of the interlobular septa together with infiltration of mixed inflammatory cells, typically forming a dense layer around the lymphatic vessels. In affected bronchioles, migrating PMNs were observed in the respiratory epithelium and the

Table 4
Overall severity of histological lesions and extent of specific immunolabelling

Calf ID (group)	*dpi*	*LCr (IHC intensity)*	*RCr (IHC intensity)*	*RM (IHC intensity)*	*ACC (IHC intensity)*	*LC (IHC intensity)*	*RC (IHC intensity)*
1 (G1)	1	5 (1)	5 (2)	5 (1)	5 (1)	1 (0)	1 (0)
2 (G1)	1	4 (3)	4 (3)	5 (3)	4 (3)	0 (0)	5 (3)
3 (G1)	1	4 (2)	3 (2)	5 (2)	5 (2)	2 (1)	1 (0)
4 (G1)	4	3 (2)	4 (3)	5 (3)	5 (3)	0 (0)	1 (0)
5 (G1)	4	5 (3)	3 (2)	5 (3)	4 (2)	5 (3)	3 (1)
6 (G1)	4	3 (2)	3 (1)	4 (1)	4 (3)	3 (1)	3 (1)
7 (G1)	7	4 (3)	0 (0)	5 (3)	4 (3)	0 (0)	3 (3)
8 (G1)	7	5 (3)	4 (3)	5 (3)	5 (3)	5 (3)	5 (3)
9 (G1)	7	4 (3)	2 (0)	3 (1)	1 (0)	2 (1)	2 (1)
10 (G1)	10	4 (4)	5 (4)	4 (3)	4 (4)	1 (0)	4 (4)
11 (G1)	10	4 (4)	5 (4)	5 (4)	5 (4)	0 (1)	5 (4)
12 (G1)	10	5 (4)	4 (4)	5 (4)	5 (4)	5 (4)	5 (4)
13 (G2)	1	1	0	1	1	0	0
14 (G2)	1	1	2	1	2	1	0
15 (G2)	1	1	0	0	1	0	0
16 (G2)	4	1	1	1	1	0	0
17 (G2)	4	0	0	0	0	0	0
18 (G2)	4	0	0	0	0	0	0
19 (G2)	7	1	1	0	1	0	0
20 (G2)	7	0	0	0	0	0	0
21 (G2)	7	0	0	0	0	0	0
22 (G2)	10	2	2	2	1	2	1
23 (G2)	10	0	0	0	0	0	1
24 (G2)	10	0	0	0	0	2	0

Histological lesions and immunolabelling both scored 0–5 where 0 = no significant lesions/labelling and 5 = most severe lesions/prominent labelling. Scores were assigned to individual lung lobes for each calf. G1, calves infected with *P. multocida* A:3; G2, calves administered sterile saline (negative control). LCr, left cranial lung lobe; RCr, right cranial lung lobe; RM, right middle lung lobe; ACC, accessory lung lobe; LC, left caudal lung lobe; RC, right caudal lung lobe. Numbers in parentheses are intensity of specific immunolabelling of *P. multocida* A:3. Specific immunolabelling was absent in all calves from G2.

associated BALT appeared hyperplastic. Subpleural fibrin was abundant.

In three G1 calves examined at 7 dpi microscopical lesions of severe suppurative bronchopneumonia were present in one or more lung lobes. Lesions were most severe in the left apical lung lobes and to a lesser extent in the right middle and accessory lung lobes (Table 4). The histological lesions were similar to those found in calves from G1 examined at 4 dpi except that the changes in the lung parenchyma were more focal, with distinct concentric layers consisting of liquifactive and coagulative necrosis,

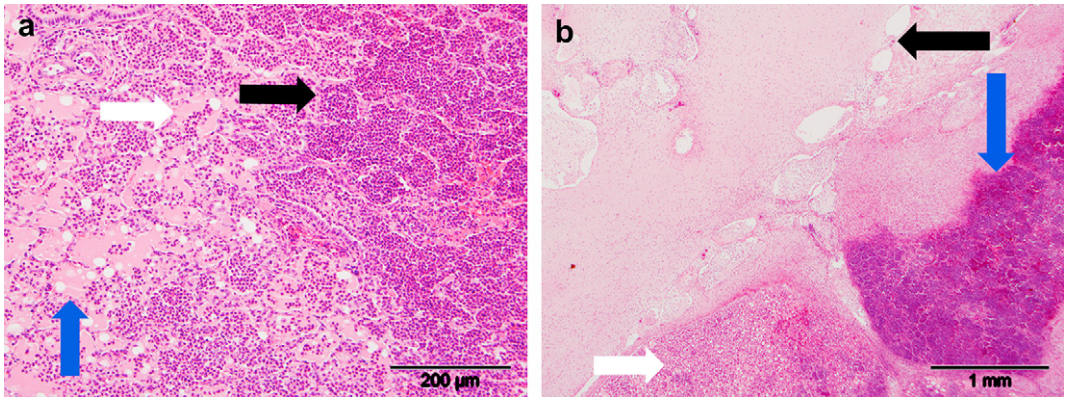

Fig. 2. (a) Lung parenchyma at 1 dpi with *P. multocida* A:3 pneumonia. Alveolar airspaces in affected areas are infiltrated with either PMNs (black arrow) or are oedematous (blue arrow) or contain a mixture of both changes (white arrow). HE. (b) Lymphatics within the interlobular septa adjacent to affected alveoli are infiltrated with either PMNs (blue arrow) or are oedematous (white arrow) or are severely dilated and oedematous (black arrow) at 1 dpi. HE.

Fig. 3. Necrotic foci, as denoted by a dense layer of PMNs and mononuclear inflammatory cells (arrow), within the lung parenchyma at 4 dpi. Note the surrounding tissue is also heavily infiltrated by PMNs or is oedematous or affected by a combination of the two processes. HE.

cell debris and fibrin centrally surrounded by a dense layer of mixed, predominantly PMNs, inflammatory cells, which in turn was surrounded by a further layer of predominantly macrophage-like inflammatory cells. Finally, a layer of relatively loose fibrous tissue, frequently incomplete, was present, which appeared to extend from interlobular septa adjacent to the lesions (Fig. 4a). The morphology was consistent with sequestra formation. The alveoli and bronchioles adjacent to these lesions contained a mixed inflammatory cell infiltrate comprised principally of PMNs, but also notable numbers of activated macrophages. The lymphatics were dilated to a slightly lesser degree than at 4 dpi, but now contained many thrombi in addition to a mixed inflammatory cell infiltrate comprised mainly of PMNs and macrophages (Fig. 4b). Subpleural oedema was present, but contained less fibrin than at 4 dpi.

At 10 dpi all of the three calves in G1 had severe or very severe lesions present in all lung lobes except for two left caudal lung lobes (Table 4). The lesions were of a similar nature to those seen at 7 dpi, but the organization around the foci of necrosis was more distinct, with fibrous tissue often totally encapsulating the lesions characteristic of abscessation. The individual inner layers of the abscesses were thicker than those at 7 dpi (Fig. 5) and the fibrous capsules of many coalesced with adjacent abscesses. Fibrin was present in some alveoli in the surrounding parenchyma and these often also contained mononuclear cells and some multinucleate giant cells. The interstitial tissue of the interlobular septa was oedematous, but to a lesser extent than at 7 dpi, and very few thrombi were present in the lymphatics, which were also less dilated. Scattered alveoli and bronchioles contained PMNs and macrophages similar to lesions found at 1 and 4 dpi.

In calves from G2 at 1 dpi there were occasional small clusters of PMNs and/or mononuclear inflammatory cells in individual or small numbers of alveoli or small bronchiole(s) in several of the lung lobes, which were otherwise normal. At 4 dpi the frequency of such findings in control calves was less and, when present, comprised occasional small interstitial foci of mononuclear inflammatory cells with few, if any, PMNs. Similar minor and sparse lung lesions were present in G2 calves at 7 and 10 dpi (Table 4).

A moderate to very severe mixed lymphadenitis was present in all of the four pulmonary lymph nodes from each of the three G1 calves examined at 1 dpi.

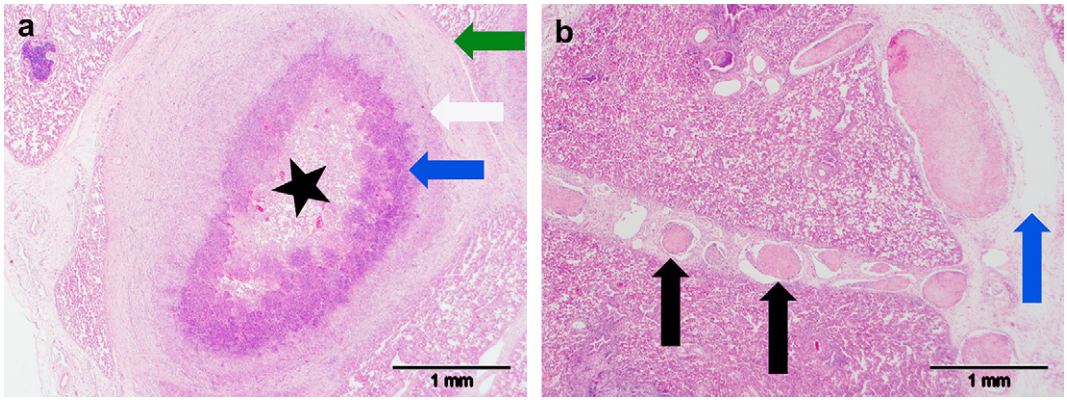

Fig. 4. (a) At 7 dpi sequestra form within the affected lung parenchyma, with multifocal lesions each comprised of a central area of liquifactive and coagulative necrosis (black star) surrounded respectively by a dense layer of PMNs (blue arrow), a dense layer of mononuclear inflammatory cells (white arrow) and finally a layer of loose fibrous tissue (green arrow). HE. (b) Many of the lymphatics within the interlobular septa are thrombosed or partially thrombosed (black arrows) in samples of affected lung taken at 7 dpi. Thromboses were not found in lungs examined at any other time point. Note also oedema in surrounding septal tissue (blue arrow). HE.

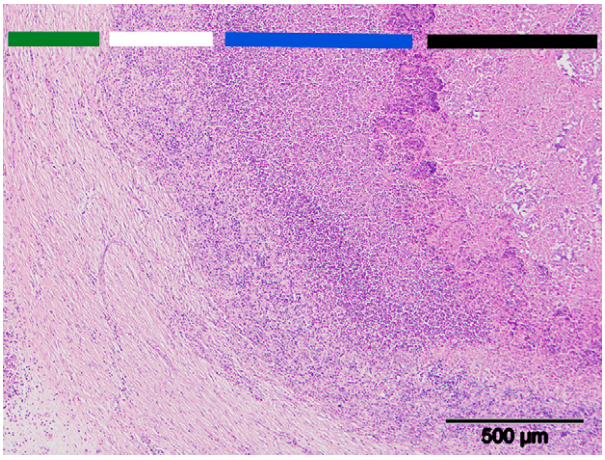

Fig. 5. Mature abscesses in the lung parenchyma of calves examined at 10 dpi. Note the concentric layers of liquifactive/coagulative necrosis (black bar), predominantly PMNs (blue bar), predominantly mononuclear inflammatory cells (white bar) all surrounded by a mature fibrous layer (green bar), which was also thicker than that first identified at 7 dpi. HE.

Large numbers of PMNs and fewer macrophages were present in the subcapsular sinuses adjacent to the trabeculae, in the medullary cords and in lesser number in the medullary sinuses. The paracortices appeared to be depleted of cells. In G2 calves at this time there was mild lymphadenitis of the left and cranial bronchial lymph nodes and one mid- and one caudal mediastinal lymph node, but the paracortices were well populated.

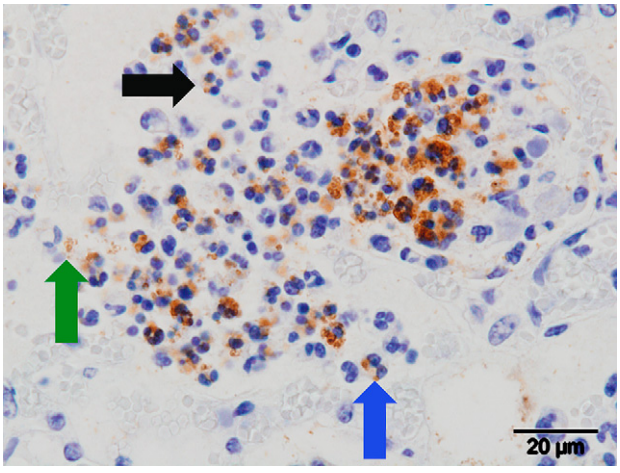

Fig. 6. Positive immunohistochemical labelling (brown) of *P. multocida* within the cytoplasm of PMNs (black arrow) and macrophages (blue arrow) in the alveoli of infected calves at 1 dpi. Note also apparent extracellular positive labelling (green arrow) suggestive of the presence of bacteria free in the alveolar airspace.

At 4 dpi all but two of the pulmonary lymph nodes examined from calves in G1 had moderate or severe lymphadenitis, which was predominantly suppurative in the left and cranial bronchial lymph nodes, yet was more mixed to non-suppurative in the mid- and caudal mediastinal lymph nodes. The cortices of all were variably depleted. No lesions were present in the pulmonary lymph nodes of G2 calves at 4 dpi.

At 7 dpi a mild–moderate predominantly suppurative lymphadenitis was present in three of the four examined pulmonary lymph nodes from one G1 calf and a mild suppurative lymphadenitis in one lymph node of another G1 calf. The other lymph nodes of calves in G1 appeared normal. No lesions were present in the pulmonary lymph nodes of calves examined from G2 at 7 dpi.

The cranial bronchial lymph nodes of all G1 calves examined at 10 dpi had a moderate mixed lymphadenitis, with plasma cells and many macrophages present in the medullary cords. A perceptible to moderate suppurative ($n = 1$) or mixed ($n = 2$) lymphadenitis was present in the caudal mediastinal lymph nodes of calves in G2, with no inflammation present in any of the other three lymph nodes examined. Depletion of the paracortex was variably present in all lymph nodes from all calves in both groups.

Immunohistochemical Labelling of P. multocida *A:3*

Labelling for *P. multocida* was present in the lungs of all calves from G1. This labelling was predominantly granular and associated with the cytoplasm of alveolar macrophages and PMNs scattered within areas of cellular infiltration (Fig. 6). This punctate labelling frequently did not completely fill the cytoplasm of the affected macrophages, but often did so in PMNs. The amount of immunolabelling between lobes was variable, yet most followed a similar pattern to the severity of the histological lung lesions (Table 4) and the mean amount of immunolabelling increased significantly ($P = 0.04$) with time. At 1 dpi there was much variation in positive labelling of bacterial antigen ranging from labelling all cells within an alveolus or group of alveoli, through to labelling only a proportion of cells within the inflammatory infiltrate, to no labelling in alveoli full of both macrophages and PMNs. Extracellular labelling was also present with the granules sometimes appearing to be in contact with the outer membranes of macrophages, lining small blood vessels or within oedematous areas in alveoli. Immunolabelling was infrequent in the interlobular septa.

At 4 dpi the immunolabelling had become more intense and was co-localized principally with histological lesions within the lung parenchyma (Fig. 7a) that

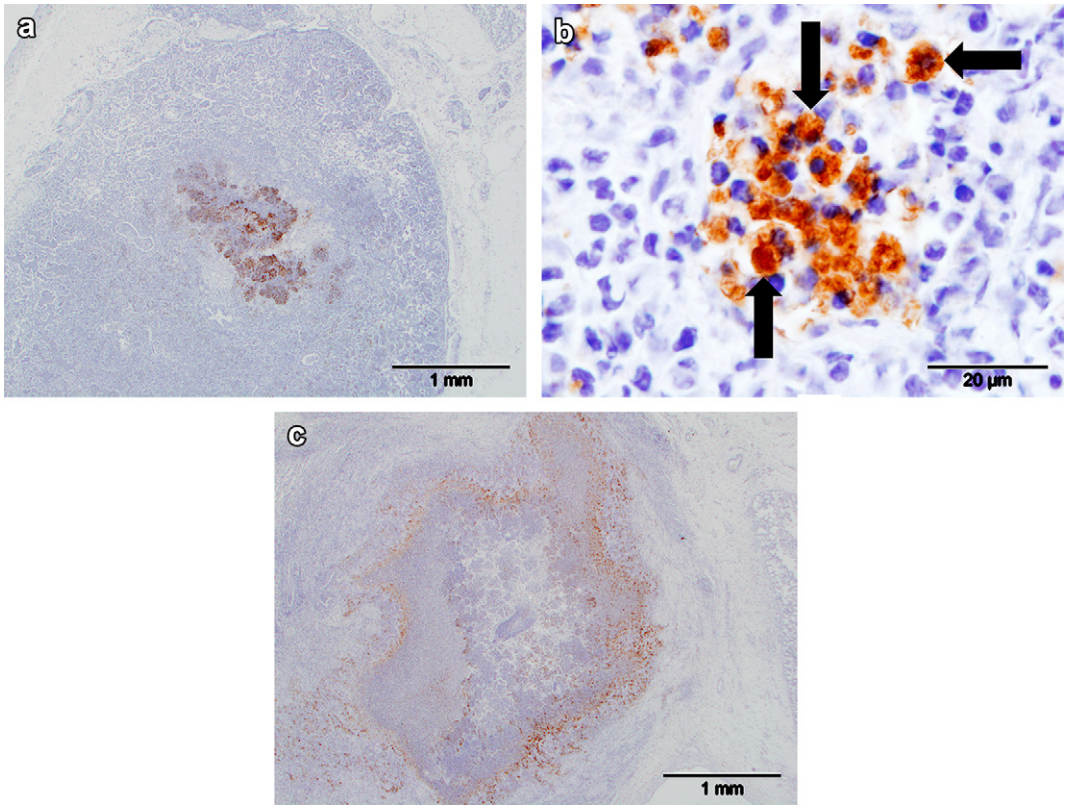

Fig. 7. (a) Immunohistochemical labelling of *P. multocida* (brown) predominantly within the central area of the delineated lesions found within the lung parenchyma at 4 dpi. (b) Labelling of *P. multocida* within the cytoplasm of PMNs and macrophages within the alveolar airspaces. Note the cytoplasm is completely and intensely labelled in most affected macrophages (arrows). (c) Labelling of *P. multocida* principally at the periphery of focal abscesses within the lung parenchyma at 10 dpi.

had become more delineated at this stage (see above). The cell type labelled and cellular distribution were similar to those at 1 dpi except that labelling often appeared throughout the cytoplasm of affected macrophages (Fig. 7b). Both cell-associated, principally in macrophages but also in PMNs, and extracellular labelling, occasionally within interlobular septa, were present. At 7 and 10 dpi the pattern of labelling and the cell type affected remained the same. However, the intensity of labelling increased (Table 4) and became more localized at the periphery of the forming abscesses (Fig. 7c) rather than at the centres of these lesions, as seen at 4 dpi (Fig. 7a).

Although there was some evidence of a higher proportion of animals having positive scores later in the study ($P = 0.045$), immunolabelling was very sparse in the four pulmonary lymph nodes examined in any of the calves from G1 (Table 4). This labelling was granular and was located within the cytoplasm of macrophages in either the subcapsular sinuses or deep paracortices. At 7 dpi all calves had a least one positively labelled affected pulmonary lymph node and the number affected rose slightly by 10 dpi (Table 3). No positive labelling was detected in any tissue, lung or lymph node, from any of the calves in G2 or any negative control preparations from calves in G1.

Discussion

This study reports, for the first time, the progression of gross and microscopical pulmonary lesions in the peracute, acute and subacute stages of pneumonic pasteurellosis in calves infected experimentally with *P. multocida* A:3. Additionally, correlations with the onset and duration of selected clinical signs and the distribution of *P. multocida* within the lesions as they developed have been demonstrated.

Extensive consolidation of the parenchyma of multiple lung lobes occurred rapidly (within 24 h of infection) in G1 calves, but not in G2 calves sham infected at the same time (Table 2). Clinically, demeanour gave little evidence of this major effect, and although rectal temperature and respiratory rates both increased in the affected animals, there was little indication of the extent of the pathological changes. This

highlights the difficulty of identifying the point at which treatment, such as antimicrobial therapy, is required to prevent significant tissue damage, particularly in housed calves not subject to much exercise. The induction and distribution of the lesions after delivering a large number of bacteria at a single time point directly to the lungs at the level of the tracheal bifurcation, thereby by-passing all upper respiratory tract defences, was likely more rapid than would occur during natural infection. Furthermore, this procedure disperses significant numbers of bacteria to some of the more caudal lung lobes, which are not typically affected during natural air-borne bacterial infections (Caswell and Williams, 2007). However, the overall pathological changes and clinical responses reflect in large measure the natural disease, and these findings have practical relevance.

The consistent involvement of the right cranial lung lobe (Tables 1 and 4), which is supplied with air via the tracheal bronchus, is noteworthy given that infection cultures were deposited immediately above the tracheal bifurcation and distal to the tracheal bronchus. The entry to the tracheal bronchus in ruminants and pigs occurs on the ventro-lateral aspect of the trachea proximal to the tracheal bifurcation (Dyce *et al*., 1996) and has a relatively small opening, approximately 5 mm diameter or less in the age and breed of calves used in this study, and a first assumption may be that this anatomical arrangement would make it unlikely that a significant amount of inoculum would enter the lobe directly. However, previous studies have shown that right cranial lung lobes supplied by tracheal bronchi are predisposed to inhalation of foreign material, especially liquids, as well as the accumulation of inflammatory exudates from the more distal lung fields as they are cleared by the mucociliary apparatus and transported up the trachea (Caswell and Williams, 2007). Therefore, it is not uncommon for this lobe to be involved extensively in inhalation pneumonia or bronchopneumonia due to air-borne bacterial infections. The mild coughing associated with the infection procedure (Dowling *et al*., 2002) and drainage of the instilled inoculum from the bronchi supplying the lung lobes distal to the tracheal bifurcation may have resulted in some bacteria entering the tracheal bronchus directly. By comparison calves infected with *M. haemolytica* via the intravenous route also developed consistent fibrinosuppurative bronchopneumonia in the right cranial lung lobe (Thomas *et al*., 1989) and the authors concluded that haematogenous spread of bacteria was an important feature in this naturally acquired disease. However, no evidence of bacteraemia has been observed with the current experimental model (Dowling, 2003), but a contributory feature may be that the anatomy of the right cranial lung lobe provides less efficient defence mechanisms compared with the others. For example, the tracheal bronchus lies in an almost vertical plane compared with the mainstem bronchi supplying the other lung lobes, in which mucociliary clearance is aided, not impeded, by gravity and, in combination with the small diameter of the tracheal bronchus, this may also compromise the efficacy of clearance of foreign material by the cough mechanism. Added to this, mucus cleared from any of the other lobes may enter the tracheal bronchus as it is transported proximally up the trachea.

Microscopical examination of lung consolidation showed that this was due to a combination of both cellular infiltration and oedema. At 1 dpi the cellular infiltration was composed primarily of PMNs that had migrated into the lower airways, especially the alveoli. Complement, chemokines and cytokines are chemotactic for PMNs and are released in response to alveolar injury and bacterial chemotactic factors such as toxins or lipopolysaccharide may also act in this fashion (López, 2001). Macrophages are key mediators of PMN chemotaxis (Hodgson, 2006) and positive cytoplasmic and the apparent surface immunolabelling of *P. multocida* on alveolar macrophages depict the stages of phagocytosis that would have initiated such signalling.

The alveolar oedema present at 1 dpi may have been an endothelial inflammatory response affecting capillaries and post-capillary venules due to cytokines released by activated macrophages and/or recruited PMNs, or it may have resulted from physical damage to blood vessels during the mass diapedesis of PMNs and monocytes/macrophages from the blood through the pulmonary post-capillary venules. However, pulmonary haemorrhages were both minor and scarce so the amount of vascular damage was not as severe as that found in pneumonic pasteurellosis caused by *M. haemolytica*, where pulmonary haemorrhages and severe pulmonary oedema, denoted by extensive and sometimes exclusive flooding of the alveoli, especially in the per-acute phase of the disease, are common (Allan *et al*., 1985). Necrosis of the vascular components was not a major feature in the present study except for the alveolar capillaries within the focal areas of inflammation in the lung parenchyma, which later became abscesses. This is in contrast to the fibrinous inflammation of the intima of pulmonary venules, hypertrophy and necrosis of the endothelium together with infiltration of PMNs into the walls of the vessels seen after experimental *M. haemolytica* infection (Jericho, 1989). The outcome of vascular damage progressed during this study from the initial alveolar oedema at 1 dpi to the presence of

fibrin, which was a major component at 4 dpi. The presence of fibrin, together with the more focal nature of the cellular lesions in the parenchyma, allowed clear differentiation from animals examined at 1 dpi. The destruction of alveolar capillaries that were within the focal areas of necrosis that began to develop at 4 dpi was due probably to the release of cytotoxic components from activated and effete PMNs and/or macrophages such as respiratory burst products and various enzymes such as elastase and lysozyme (Hodgson, 2006).

The nature of the lesions changed further by 7 dpi, first due to the presence of thrombi, which were found only within the lymphatics of the interlobular septa at this time point, and, secondly, due to formation of multiple abscesses containing discernable concentric layers of necrosis and different inflammatory cells, plus loose fibrous tissue and some mineralization. These changes were distinct from the lung lesions present at 4 dpi. At 10 dpi these layers within the abscesses were more distinctive and the fibrous tissue was mature. Multiple abscessation is another discriminatory feature of pneumonia caused by *P. multocida* A:3 in cattle compared with that caused by *M. haemolytica* (Allan *et al.*, 1985).

Immunohistochemical labelling for *P. multocida* in the lungs showed the bacteria to be mainly intracytoplasmic and granular in both PMNs and macrophages and always associated with histological lesions. However, the cytoplasmic distribution of labelling at 1 dpi in the two cell types differed in that frequently the whole of the cytoplasm was labelled positively in PMNs, but usually only partially in macrophages. This suggests differing roles for, or different rates of killing by, the two cell types, with PMNs ingesting larger numbers of bacteria, which would help reduce bacterial replication and any deleterious effects on the surrounding tissues. The macrophages, however, appeared to have the bacteria sequestered within discrete intracytoplasmic compartments, presumably phagolysosomes for processing and antigen presentation. This would explain the presence of labelled macrophages, but not PMNs, in the draining lymph nodes. Why the intracytoplasmic distribution of labelling had altered by 4 dpi, with a greater proportion appearing in macrophages compared with PMNs is unknown. The pattern of labelling within the lung lesions also changed over time, as it was localized to the centres of the early abscesses at 4 dpi but had altered to mainly the periphery of the maturing abscesses at 7 and 10 dpi. It is tempting to speculate that by 7–10 dpi, as the abscesses matured, the antigens at the centres had been removed and processed by macrophages and PMNs and therefore were no longer recognized by the polyclonal anti-*P. multocida* antibodies. In contrast, bacteria at the periphery of the lesions may have been at an earlier stage of interaction with immune cells.

The practical implication of this work relates to the observation that significant irreversible damage to the lung may occur during the early stages of pneumonic pasteurellosis. This is clearly seen from the detection of an inflammatory response as early as 1 dpi, with commencement of abscess formation within 4 dpi. Although the lesions in experimental and naturally acquired pneumonia caused by *P. multocida* A:3 are similar, it is not known if they develop over comparable timescales. The onset of clinical signs in the naturally acquired disease may be more subtle than observed in this study, especially in the peracute stages, thereby reducing the likelihood of timely recognition. The treatment for bacterial bovine pneumonia is administration of antimicrobials, many of which have been found to be ineffective, especially against *P. multocida* actually recovered from pneumonic cattle (Clavijo *et al.*, 2002). Even antimicrobials with high in-vitro efficacy (Catry *et al.*, 2002) cannot be relied upon to penetrate the avascular fibrous tissue associated with abscesses in sufficient concentration (Galandiuk *et al.*, 1995), resulting in residual foci of bacteria and the potential for the disease to progress to a chronic stage once therapy has ceased. Chronic infection will result in increased incidence of permanent lung damage that is refractory to remodelling, which will, in turn, lead to loss of condition (Dalgleish, 1991), recrudescence of clinical disease and also act as a source of infection for cohorts. This study provides the foundations for the further investigation of the pathogenesis of *P. multocida* A:3 pneumonia in cattle with the ultimate goal of producing an effective vaccine.

Acknowledgments

The authors thank the members of the Bioservices Division of the Moredun Research Institute for expert care and management of the calves in this study and Dr. D. Buxton for constructive criticism of the manuscript. The work was funded by the Scottish Government.

References

Allan EM, Gibbs HA, Wiseman A, Selman IE (1985) Sequential lesions of experimental bovine pneumonic pasteurellosis. *Veterinary Record*, **117**, 438–442.

Biberstein EL (1990) Our understanding of the Pasteurellaceae. *Canadian Journal of Veterinary Research*, **54**, S78–S82.

Caswell JL, Williams KJ (2007) Respiratory system. In: *Jubb, Kennedy and Palmer's Pathology of Domestic Animals*,

MG Maxie, Ed., Saunders Elsevier, London, pp. 523–653.

Catry B, Govaere JLJ, Devriese L, Laevens H, Haesebrouck F *et al*. (2002) Bovine enzootic bronchopneumonia: prevalence of pathogens and their antimicrobial susceptibility. *Vlaams Diergeneeskundig Tijdschrift*, **71**, 348–354.

Clavijo AM, Alfaro C, Rolo M, Diaz C, Santander J *et al*. (2002) Resistance and sensibility to antimicrobials in *Pasteurella multocida* strains isolated from calves with pneumonia in Monagas state, Venezuela. *Revista Cientifica-Facultad de Ciencias Veterinarias*, **12**, 626–629.

Confer AW, Nutt SH, Dabo SM, Panciera RJ, Murphy GL (1996) Antibody responses of cattle to outer membrane proteins of *Pasteurella multocida* A:3. *American Journal of Veterinary Research*, **57**, 1453–1457.

Dalgleish R (1989) *Studies on Experimental Pneumonia Pasteurellosis in Calves*. PhD thesis, University of Glasgow.

Dalgleish R (1991) Differential diagnosis of respiratory disease in adult cattle. *In Practice*, **13**, 237–241.

Dowling AA (2003) *Pathophysiological Investigations of Pneumonic Pasteurellosis due to* Pasteurella Multocida *type A:3 in Calves*. PhD thesis, University of Glasgow.

Dowling A, Hodgson JC, Dagleish MP, Eckersall PD, Sales J (2004) Pathophysiological and immune cell responses in calves prior to and following lung challenge with formalin-killed *Pasteurella multocida* biotype A: 3 and protection studies involving subsequent homologous live challenge. *Veterinary Immunology and Immunopathology*, **100**, 197–207.

Dowling A, Hodgson JC, Schock A, Donachie W, Eckersall PD *et al*. (2002) Experimental induction of pneumonic pasteurellosis in calves by intratracheal infection with *Pasteurella multocida* biotype A: 3. *Research in Veterinary Science*, **73**, 37–44.

Dyce KM, Sack WO, Wensing CJG (1996) The respiratory apparatus. In: *Textbook of Veterinary Anatomy*, WB Saunders, London, pp. 151–168.

Galandiuk S, Lamos J, Montgomery W, Young S, Polk HC (1995) Antibiotic penetration of experimental intra-abdominal abscesses. *American Surgeon*, **61**, 521–525.

Gilmour NJL, Martin WB, Sharp JM, Thompson DA, Wells PW *et al*. (1983) Experimental immunization of lambs against pneumonic pasteurellosis. *Research in Veterinary Science*, **35**, 80–86.

Gourlay RN, Thomas LH, Wyld SG (1989) Experimental *Pasteurella multocida* pneumonia in calves. *Research in Veterinary Science*, **47**, 185–189.

Hodgson JC (2006) Endotoxin and mammalian host responses during experimental disease. *Journal of Comparative Pathology*, **135**, 157–175.

Ishiguro K, Kitajima T, Kubota S, Amimoto K, Oda K *et al*. (2005) Experimental infection of calves with *Pasteurella multocida* serovar A:3 isolated in Japan. *Journal of Veterinary Medical Science*, **67**, 817–819.

Jericho KWF (1989) Histological changes in lungs of calves exposed to an aerosol of *Pasteurella haemolytica*. *Journal of Comparative Pathology*, **101**, 87–99.

López A (2001) Respiratory system, thoracic cavity and pleura. In: *Thomson's Special Veterinary Pathology*, MD McGavin, WW Carlton, JF Zachary, Eds., Mosby, St Louis, pp. 125–195.

Mathy NL, Mathy JPD, Lee RP, Walker J, Lofthouse S *et al*. (2002) Pathological and immunological changes after challenge infection with *Pasteurella multocida* in naive and immunized calves. *Veterinary Immunology and Immunopathology*, **85**, 179–188.

Rimler RB, Rhoades KR (1989) *Pasteurella multocida*. In: *Pasteurella and Pasteurellosis*, C Adlam, JM Rutter, Eds., Academic Press, London, pp. 37–73.

Thomas LH, Gourlay RN, Wyld SG, Parsons KR, Chanter N (1989) Evidence that blood-borne infection is involved in the pathogenesis of bovine pneumonic pasteurellosis. *Veterinary Pathology*, **26**, 253–259.

Townsend KM, Frost AJ, Lee CW, Papadimitriou JM, Dawkins HJS (1998) Development of PCR assays for species- and type-specific identification of *Pasteurella multocida* isolates. *Journal of Clinical Microbiology*, **36**, 1096–1100.

Veterinary Laboratories Agency. (2007) *VIDA 2007, Yearly Trends, Cattle*. http://www.defra.gov.uk/vla/reports/rep_vida07.htm.

Weekley LB, Veit HP, Eyre P (1998) Bovine pneumonic pasteurellosis. Part I. Pathophysiology. *Compendium on Continuing Education for the Practicing Veterinarian*, **20**, S33–S46.

[*Received, March 17th, 2009*
Accepted, October 13th, 2009]